Optimum Configurations for Single-Amplifier Biquadratic Filters

ADEL S. SEDRA, MEMBER, IEEE, MOHAMED A. GHORAB, MEMBER, IEEE, AND KEN MARTIN, MEMBER, IEEE

Abstract—Two new biquad circuits based on the Sallen–Key positive feedback structure are introduced and shown to be capable of realizing all possible second-order filter functions. The pole design equations and pole sensitivities are identical to those of the Deliyannis bandpass circuit which is the basis for the Friend biquad. The new circuits, however, display lower transmission zero sensitivities than the Friend notch realizations. Design details and experimental results are given.

I. Introduction

CIRCUITS which utilize a single op amp and an RC network to realize a second-order voltage transfer function offer a low-cost and low-power approach to the design of active-RC filters. These single amplifier biquads, or SAB's, can be used either in cascade or in a low-sensitivity coupled structure [1], [2] to realize a given high-order filter transfer function. Over the last decade or so, considerable effort has been directed towards finding the "best" SAB circuit realization [2]–[6]. A particular circuit emerged as having highly desirable properties. This circuit was first reported by Deliyannis [7] for the realization of bandpass functions and was subsequently generalized by Friend [8] for the realization of other filtering functions. These efforts resulted in the popular STAR building block [9].

A method for the optimum design of the Deliyannis bandpass circuit was provided by Fleischer [10]. His work, and the recent work on the classification of SAB's [11], have shown that the Deliyannis circuit uses both negative and positive feedback to obtain the required selectivity. The sensitivity performance of the circuit can, therefore, be optimized to suit a given realization technology by choosing the proper mix of the two feedback polarities. This flexibility is the key to the popularity of the Deliyannis circuit and of its descendent the Friend biquad.

The Deliyannis bandpass circuit, shown in Fig. 1, uses a bridged-T RC network in the negative feedback path of the op amp together with the resistive positive feedback. To obtain other filtering functions, Friend [8] loaded the bridged-T network. This still did not enable the realization of the low-pass function, which was obtained [9] using another circuit configuration.[1] Loading the bridged-T network complicates the design process and does not enable the direct application of Fleischer's results on optimizing the design.

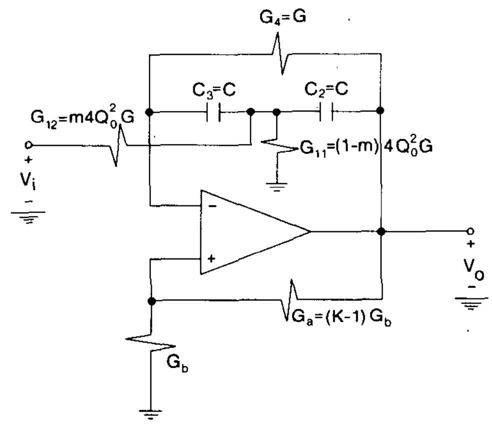

Fig. 1. The Deliyannis bandpass circuit.

Recent work on the application of the complementary transformation to active network design [11], [12] has shown that the complement of the Deliyannis circuit is the Sallen–Key positive feedback structure. Since the complementary transformation preserves the circuit poles and their sensitivities, it became apparent that one should be able to design the Sallen–Key positive feedback circuit to have identical pole sensitivities as that obtained in the Deliyannis circuit. Furthermore, once the Deliyannis circuit has been optimized, the complementary transformation will result in an optimum design of the Sallen–Key circuit. Since the complementary transformation does not preserve the transmission zeros, the question arose as to whether filtering functions other than bandpass (which is most conveniently implemented using the Deliyannis circuit) could be advantageously realized using the Sallen–Key positive feedback structure. The answer to this question turned out to be an affirmative one. All the special biquad functions except the bandpass, can be most conveniently realized using the Sallen–Key positive feedback structure. The resulting circuits have identical pole sensitivities as those of the Deliyannis circuit. The sensitivities of the transmission zeros, however, are superior to those obtained with Friend's notch circuits.

The purpose of this paper is to present the circuits and optimum design of the biquads obtained from the Sallen–Key positive feedback structure. The special cases of low- and high-pass circuits are well known, the notch and

Manuscript received September 27, 1979; revised April 22, 1980. This work was supported in part by the Natural Sciences and Engineering Research Council under Grant A7394.

A. S. Sedra is with the Department of Electrical Engineering, University of Toronto, Toronto, Ont., Canada M5S 1A4.

M. A. Ghorab is with the Department of Electrical Engineering, Ryerson Polytechnical Institute, Toronto, Ont., Canada.

K. Martin was with the Department of Electrical Engineering, University of Toronto, Canada. He is now with the Department of Electrical Sciences and Engineering, University of California, Los Angeles, CA 90024.

[1] This other configuration is based on loading the "dual" bridged-T network, in the circuit of Fig. 2(c), at the node between the two resistors.

0098-4094/80/1200-1155$00.75 © 1980 IEEE

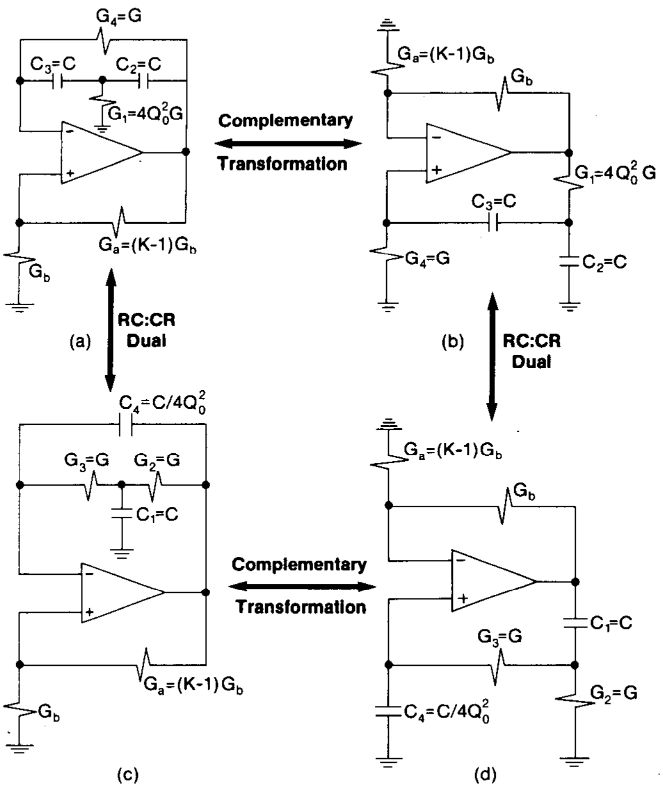

Fig. 2. Feedback structures for (a) the Deliyannis circuit, (b) its complement, (c) its RC "dual", and (d) the complement of the circuit in (c). The circuits in (a) and (c) are of the enhanced negative feedback (ENF) class and those in (b) and (d) are of the enhanced positive feedback (EPF) class.

all-pass realizations, however, are thought to be new. In summary we shall present the optimum circuit configuration and design for each of the different second-order filter functions.

II. Circuit Generation

A. Feedback Structures

Fig. 2(a) shows the feedback structure of the Deliyannis circuit, obtained by simply grounding the input terminal of the circuit in Fig. 1, with $G_1 = G_{11} + G_{12}$. To realize a pair of complex-conjugate poles characterized by a frequency ω_0 and a Q-factor Q, the design equations are

$$\frac{C}{G} = \frac{2Q_0}{\omega_0} \tag{1}$$

$$K-1 = \frac{1}{2Q_0^2}\left(1 - \frac{Q_0}{Q}\right) \tag{2}$$

where the value of G (or C) and of G_b can be chosen arbitrarily, and where Q_0 is a design parameter ($Q_0 \leqslant Q$). The choice of optimum value for Q_0 is discussed in Section III. For the time being note that the parameter K determines the amount of positive feedback. In the limit when $K=1$ the circuit degenerates to the familiar multiple-feedback realization. In this degenerate case, the poles realized have a quality factor equal to the parameter Q_0. Applying positive feedback, that is making $K>1$, moves the poles (on a circular locus) closer to the $j\omega$-axis. Thus the poles acquire a quality factor $Q > Q_0$, while the pole frequency ω_0 remains unchanged. This process is referred to as Q-enhancement, and the circuit of Fig. 2(a) has been classified [11] as an enhanced negative-feedback (ENF) configuration.

Using the "dual" bridged-T network results in the circuit of Fig. 2(c). This latter circuit has identical poles, pole sensitivities and pole design equations as the circuit of Fig. 2(a). Similar to the circuit of Fig. 2(a) this circuit is only capable of realizing bandpass and all-pass functions.[2]

Fig. 2(b) shows the circuit obtained by applying the complementary transformation to the circuit of Fig. 2(a). Similarly, application of the complementary transformation to the circuit of Fig. 2(c) results in the circuit of Fig. 2(d). Briefly, the process of applying the complementary transformation consists of interchanging the op amp output terminal with ground. That is, terminals of the feedback networks which were connected to the op amp output should be now grounded, and vice versa. In addition, the op amp input terminals should be interchanged.

It can be easily observed that the circuits of Fig. 2(b) and (d) have identical feedback structures as the Sallen–Key positive feedback circuits. Since the RC network is placed in the positive feedback path and for $K>1$, the circuits of Fig. 2(b) and (d) have been classified as enhanced positive-feedback (EPF) configurations. In this classification the term positive feedback is reserved for the degenerate case obtained when $K=1$, in which case the op amp is used as a unity-gain amplifier.

Before proceeding any further we wish to reiterate the fact that all the circuits in Fig. 2 have the same poles, pole sensitivities and pole design equations ((1) and (2)).

B. Transmission Zeros

We now consider the use of the two EPF structures of Fig. 2(b) and (d) in the realization of transfer functions of the form

$$T(s) = \frac{n_2 s^2 + n_1 s + n_0}{s^2 + s\left(\dfrac{\omega_0}{Q}\right) + \omega_0^2} \tag{3}$$

where the numerator coefficients n_0, n_1, and n_2 determine the transmission zeros and hence the type of filtering function. To accomplish this task without changing the circuit poles, every component connected to ground may be partially or fully lifted off ground and connected to the input signal source. The resulting circuits, to be referred to as high-pass biquad (HPB) and low-pass biquad (LPB) are shown in Fig. 3(a) and 3(b), respectively. As will be now shown, each of these two biquads is capable of realizing the general second-order filter transfer function of (3).

Analysis of the HPB circuit of Fig. 3(a), assuming the op amp to be ideal, results in a transfer function of the

[2] The bandpass filter is obtained by injecting the input signal through part or all of the capacitance C_1. The all-pass function is obtained by injecting the input signal through part of C_1 and through part of G_b.

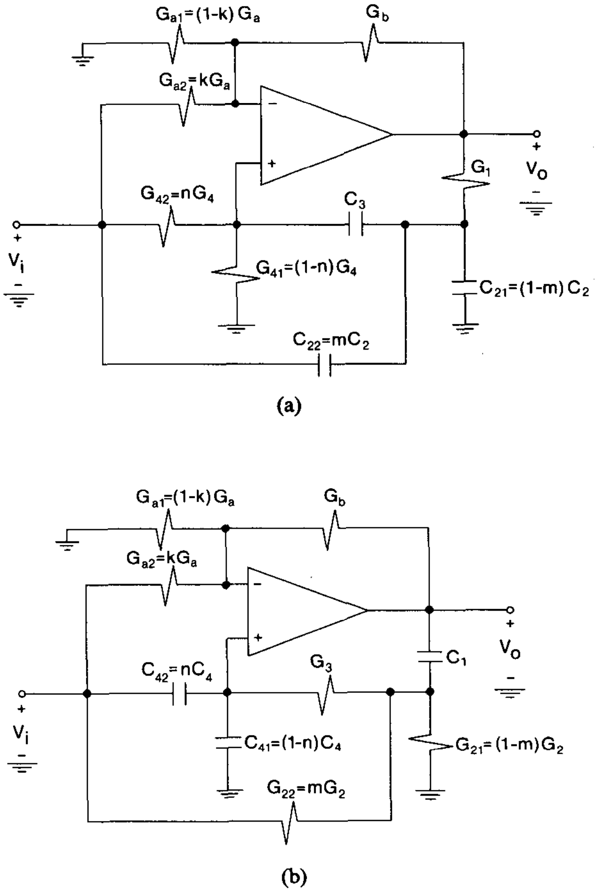

Fig. 3. The two new circuits: (a) high-pass biquad (HPB), based on the structure of Fig. (2b), and (b) low-pass biquad (LPB), based on the structure of Fig. (2d). For design data see Table I.

form in (3) with the various coefficients given by

$$\omega_0^2 = \frac{G_1(G_{41}+G_{42})}{C_3(C_{21}+C_{22})} \tag{4}$$

$$\frac{\omega_0}{Q} = (G_{41}+G_{42})\left(\frac{1}{C_{21}+C_{22}}+\frac{1}{C_3}\right) - \left(\frac{G_1}{C_{21}+C_{22}}\right)\left(\frac{G_{a1}+G_{a2}}{G_b}\right) \tag{5}$$

$$n_2 = \left(\frac{G_{a1}+G_{a2}+G_b}{G_b}\right)\left(\frac{C_{22}}{C_{21}+C_{22}}\right) - \left(\frac{G_{a2}}{G_b}\right) \tag{6}$$

$$n_1 = \left(\frac{G_{a1}+G_{a2}+G_b}{G_b}\right)G_{42}\left(\frac{1}{C_{21}+C_{22}}+\frac{1}{C_3}\right) - \left(\frac{G_{a2}}{G_b}\right) \cdot \left[\frac{G_1}{C_{21}+C_{22}} + (G_{41}+G_{42})\left(\frac{1}{C_{21}+C_{22}}+\frac{1}{C_3}\right)\right] \tag{7}$$

$$n_0 = \frac{G_1(G_{41}+G_{42})}{C_3(C_{21}+C_{22})} \cdot \left[\left(\frac{G_{42}}{G_{41}+G_{42}}\right)\left(\frac{G_{a1}+G_{a2}+G_b}{G_b}\right) - \left(\frac{G_{a2}}{G_b}\right)\right]. \tag{8}$$

Similarly, analysis of the LPB circuit of Fig. 3(b), assuming the op amp to be ideal, results in a transfer function whose coefficients are given by

$$\omega_0^2 = \frac{G_3(G_{21}+G_{22})}{C_1(C_{41}+C_{42})} \tag{9}$$

$$\frac{\omega_0}{Q} = \left(\frac{G_{21}+G_{22}+G_3}{C_1}\right) - \left(\frac{G_3}{C_{41}+C_{42}}\right)\left(\frac{G_{a1}+G_{a2}}{G_b}\right) \tag{10}$$

$$n_2 = \left(\frac{G_{a1}+G_{a2}+G_b}{G_b}\right)\left(\frac{C_{42}}{C_{41}+C_{42}}\right) - \left(\frac{G_{a2}}{G_b}\right) \tag{11}$$

$$n_1 = \left(\frac{G_{a1}+G_{a2}+G_b}{G_b}\right)\left(\frac{C_{42}}{C_{41}+C_{42}}\right)\left(\frac{G_{21}+G_{22}+G_3}{C_1}\right) - \left(\frac{G_{a2}}{G_b}\right)\left(\frac{G_3}{C_{41}+C_{42}}+\frac{G_{21}+G_{22}+G_3}{C_1}\right) \tag{12}$$

$$n_0 = \frac{G_3(G_{21}+G_{22})}{C_1(C_{41}+C_{42})}\left[\left(\frac{G_{22}}{G_{21}+G_{22}}\right)\left(\frac{G_{a1}+G_{a2}+G_b}{G_b}\right) - \left(\frac{G_{a2}}{G_b}\right)\right]. \tag{13}$$

Table I provides complete design equations which enable obtaining a *nominal* design for each of the six special cases of the second-order transfer function. It should be noted that in the third column of Table I one of the two biquads is suggested as the preferred realization. This preference is based on the sensitivity of the transmission zeros. Thus though the HPB is capable of realizing notch functions for any value of (ω_z/ω_0), the sensitivities of the zero frequency ω_z and of the notch depth increase as the ratio (ω_z/ω_0) increases. Therefore, HPB is more suitable for realizing high-pass notch (and obviously high-pass) transfer functions. The opposite is true for LPB making it suitable for the low-pass notch (and low-pass) case. As indicated in Table I either of two biquads can be used to realize the all-pass function. On the other hand, the band-pass function is most conveniently realized using the Deliyannis circuit of Fig. 1.

The design equations of Table I are based on the choice of a suitable value for the design parameter Q_0. This is a free parameter whose value controls the pole sensitivities as explained in the next section. In using Table I, it should be noted that the component split coefficients k, n, and m are defined on the circuit diagrams of Fig. 3.

Finally, it should be mentioned that the nominal designs of Table I will require nondiscrete values for the capacitors. This practical difficulty can be alleviated by considering this design only as an initial one and following the step-by-step design procedure given in Section IV. This latter design procedure also includes predistortion for the effects of the limited frequency response of the amplifier.

III. Pole Sensitivity and Design Optimization

The two new Biquads have the same poles and pole sensitivities as the Deliyannis circuit. Thus the work done on the selection of optimum value of Q_0 for the Deliyannis circuit can be directly applied to the new circuits. In

TABLE I
NOMINAL DESIGN EQUATIONS FOR THE TWO BIQUADS OF FIG. 3 AND THE DELIYANNIS CIRCUIT OF FIG. 1

Transfer Function: $T(s) = N(s)/[s^2 + s(\frac{\omega_o}{Q}) + \omega_o^2]$

For all circuits

* Choose a value for $Q_o < Q$ from sensitivity and technology considerations [section (3)]
* $G_a = (K-1)G_b$, where $K - 1 = \frac{1}{2Q_o^2}(1 - \frac{Q_o}{Q})$ and G_b arbitrary

For HPB and Deliyannis Circuit:

$G_1 = 4Q_o^2 G$, $G_4 = G$, $C_2 = C_3 = C$, $\frac{G}{C} = \frac{2Q_o}{\omega_o}$, where G or C is arbitrary

For LPB

$G_2 = G_3 = G$, $C_1 = C$, $C_4 = C/4Q_o^2$, $(G/C) = (2Q_o/\omega_o)$, where G or C is arbitrary

* The constants k, m and n (each ≤ 1) should be selected as follows

Filter Type	N(s)	Preferrable Circuit	k	n	m	Notes
Low Pass (LP)	n_o	LPB Fig. (3b)	0	0	$n_o/K\omega_o^2$	For minimum component count, select m = 1
Bandpass (BP)	$-n_1 s$	Deliyannis Fig. (1)	0	0	$n_1/(2KQ_o\omega_o)$	
High-Pass (HP)	$n_2 s^2$	HPB Fig. (3a)	0	0	n_2/K	
Low-Pass Notch (LPN)	$n_2(s^2+\omega_z^2)$ $\omega_z \geq \omega_o$	LPB Fig. (3b)	$\frac{n_2}{(1-\frac{Q_o}{Q})}$	$k(1-\frac{Q_o}{KQ})$	$k(\frac{K-1}{K})[1+2Q_o^2(\frac{\omega_z}{\omega_o})^2]$	k determines the gain constant n_2, but should be selected to yield $m \leq 1$
High-Pass Notch (HPN)	$n_2(s^2+\omega_z^2)$ $\omega_z \leq \omega_o$	HPB Fig. (3a)	$\frac{n_2(\omega_z/\omega_o)^2}{(1-\frac{Q_o}{Q})}$	$k(1-\frac{Q_o}{KQ})$	$k(\frac{K-1}{K})[1+2Q_o^2(\frac{\omega_o}{\omega_z})^2]$	
All-Pass (AP)	$n_2(s^2-s\frac{\omega_o}{Q}+\omega_o^2)$	Either LPB or HPB	1	$[1-\frac{2}{K(1+\frac{Q}{Q_o})}]$	$[1-\frac{2}{K(1+\frac{Q}{Q_o})}]$	Gain constant n_2 is fixed: $n_2 = (Q-Q_o)/(Q+Q_o)$

this section we consider the pole sensitivities and the minimization of the pole variability through an optimum selection of Q_0. The following results apply to the two biquads of Fig. 3 and to the Deliyannis bandpass circuit of Fig. 1.

A. Active Sensitivities

The active sensitivities are measured by the gain-sensitivity product GS defined as

$$\mathrm{GS} = S_{A_0}^{Q} A_0$$

where A_0 is the dc gain of the op amp. Although evaluated at low-frequencies, the gain-sensitivity product predicts the effects of the op amp's limited bandwidth on the filter performance. For instance, if one assumes a single-pole model for the op amp, that is,

$$A(s) = \frac{A_0}{1+\frac{s}{\omega_b}} \simeq \frac{A_0\omega_b}{s} \equiv \frac{\omega_t}{s}$$

where ω_t is the unity-gain bandwidth, then it can be shown that for all the circuits in this paper the dominant pole pair undergoes a change characterized by a fractional change in ω_0 of $(\Delta\omega_0/\omega_0)$ and in Q of $(\Delta Q/Q)$ where

$$\frac{\Delta\omega_0}{\omega_0} \simeq -\frac{1}{2Q}\mathrm{GS}\left(\frac{\omega_0}{\omega_t}\right)$$

$$\frac{\Delta Q}{Q} \simeq \mathrm{GS}\left(\frac{\omega_0}{\omega_t}\right)\left(\frac{1}{2Q} - K\frac{\omega_0}{\omega_t}\right).$$

For our circuits

$$\mathrm{GS} \simeq 2Q_0 Q \tag{14}$$

leading to

$$\frac{\Delta\omega_0}{\omega_0} \simeq -Q_0\left(\frac{\omega_0}{\omega_t}\right) \tag{15}$$

$$\frac{\Delta Q}{Q} \simeq 2Q_0 Q\left(\frac{\omega_0}{\omega_t}\right)\left(\frac{1}{2Q} - \frac{\omega_0}{\omega_t}\right). \tag{16}$$

These two equations clearly indicate that the pole shift (due to the finite bandwidth of the op amp) is directly proportional to the value of Q_0. Although one can use (15) and (16) to predistort the nominal design, as will be shown below, variations in ω_t will still result in variations

TABLE II
PASSIVE SENSITIVITIES FOR THE TWO BIQUADS OF FIG. 3 AND THE DELIYANNIS CIRCUIT OF FIG. 1; THE BRACKETED PARAMETERS APPLY TO THE LOW-PASS BIQUAD (FIG. 3(b))

S — OF / w.r.t.	ω_o	Q
$R_1(C_1)$	$-\frac{1}{2}$	$-(\frac{Q}{Q_o}-\frac{1}{2})$
$C_2(R_2)$	$-\frac{1}{2}$	$-\frac{1}{2}(\frac{Q}{Q_o}-1)$
$C_3(R_3)$	$-\frac{1}{2}$	$\frac{1}{2}(\frac{Q}{Q_o}-1)$
$R_4(C_4)$	$-\frac{1}{2}$	$(\frac{Q}{Q_o}-\frac{1}{2})$
R_a	0	$-(\frac{C}{Q_o}-1)$
R_b	0	$(\frac{Q}{Q_o}-1)$

in ω_0 and Q according to the sensitivity expressions

$$S_{\omega_t}^{\omega_0} \simeq Q_0\left(\frac{\omega_0}{\omega_t}\right) \tag{17}$$

$$S_{\omega_t}^{Q} = -Q_0\left(\frac{\omega_0}{\omega_t}\right)\left[-1+4Q\left(\frac{\omega_0}{\omega_t}\right)\right]. \tag{18}$$

Thus the active sensitivities can be reduced by choosing a low value for Q_0. This, however, will result in an increase in the passive sensitivities, as shown next.

B. Passive Sensitivities

Next we consider the sensitivities of ω_0 and Q relative to all the passive elements. The results which apply to all the circuits of Fig. 1 and Fig. 3 are given in Table II. It should be mentioned that whenever an element is split for signal injection the sensitivity with respect to each of the resulting two components is a fraction of the original sensitivity value. From Table II it is clear that as Q_0 is made smaller, the passive sensitivities of Q increase. An extreme case is found in the traditional design of the Sallen–Key positive feedback circuits. For these designs $Q_0 = 0.5$ and the passive sensitivities are clearly quite high. Another extreme case is obtained in the multiple feedback circuit, in which case $K=1$, $Q_0 = Q$ and the passive sensitivities of Q are quite small. The active sensitivities, however, are quite large, as can be seen by substituting $Q_0 = Q$ in (17) and (18).

C. Optimum Selection of the Value of Q_0

The optimum value of Q_0 is that value which equilibriates the contributions to the overall variability of the transfer function of the variation in the op amp gain and bandwidth on the one hand and those of the passive components on the other hand. This value will obviously depend on the realization technology. From the sensitivity results above, and from experience, we have found that for $Q = 10-20$ a value of Q_0 in the range 3–5 is a reasonable choice.

A thorough investigation into the question of optimum value of Q_0 has been reported by Fleischer [10]. Using the variance of the fractional pole shift $\sigma^2(\Delta s/s_0)$ as a figure of merit Fleischer found that for high $Q(Q \geqslant 5)$ a near optimum design is obtained when Q_0 is selected according to

$$Q_0 = \left[|A(s_0)|^2 \frac{(8\sigma_R^2 + \sigma_C^2)}{8\sigma_A^2}\right]^{1/4} \tag{19}$$

where s_0 denotes the nominal value of the pole,

$$s_0 = -\frac{\omega_0}{2Q} + j\omega_0\sqrt{1-\frac{1}{4Q^2}}\ . \tag{20}$$

$A(s_0)$ is the gain of the op amp at s_0, and σ_R^2, σ_C^2, and σ_A^2 are the variances in the values of the resistances, capacitances, and op amp gain, respectively. It is assumed that like components have the same statistics.

The choice of Q_0 according to [19] provides the optimum balance in the tradeoff between the contributions of the passive and active component variations to the fractional pole shift. It should be noted, however, that the minimum of $\sigma^2(\Delta s/s_0)$ is quite shallow allowing that sizable departures from the optimum design, for the sake of easier realization, may be made with relative impunity.

D. Predistortion for the Effects of Finite ω_t

The bulk of the initial shift in the pole position due to the finite op amp bandwidth can be eliminated by predistorting the nominal design. For the case of a single pole op amp, this predistortion can be achieved by applying the negative of the values given by (15) and (16) to the nominal pole frequency ω_0 and quality factor Q, respectively, leading to the following expressions for the predistorted frequency ω_p and predistorted Q-factor Q_p,

$$\omega_p = \omega_0\left[1 + Q_0\left(\frac{\omega_0}{\omega_t}\right)\right] \tag{21}$$

$$Q_p = Q\left[1 - 2Q_0 Q\left(\frac{\omega_0}{\omega_t}\right)\left(\frac{1}{2Q} - \frac{\omega_0}{\omega_t}\right)\right]. \tag{22}$$

IV. DESIGN PROCEDURE

The design equations of Table I usually require nondiscrete capacitor values. In the following we provide a simple step-by-step design procedure which is based on first obtaining a nominal design using Table I and then selecting convenient standard values for all capacitors. The values of all conductances are then calculated. This procedure can be also used in a deterministic tuning process in which case measured capacitor values are used in calculating the values of the various conductances. Before presenting the design procedure we should note that sufficient degrees of freedom exist to enable designing for a given gain constant n_2 (except in the all-pass case). Nevertheless, the resulting design equations become too complex to include here. Rather, in the design procedure presented, we exhaust one of these degrees of freedom with the result that the gain constant obtained will be slightly different than the nominal value. However, the deviation in the value of gain constant is usually sufficiently small to be insignificant.

A. Design of the LPB (Fig. 3(b))

1) Choose a value for Q_0 (see Section III) and use Table I to obtain nominal values for K, k, and n.

2) Choose convenient values for C_{41}, C_{42}, and C_1 so that

$$\frac{C_{42}}{C_{41}} \simeq \frac{n}{1-n} \tag{23}$$

and

$$C_1 \simeq 4Q_0^2(C_{41}+C_{42}).$$

To ensure solvability of design equations, (C_{42}/C_{41}) should be selected smaller or equal to the value implied by (23). Note that in the low-pass case $n=0$ leading to $C_{42}=0$. If deterministic tuning in employed the capacitor values used from here on should be the measured values.

3) Determine predistorted values for the pole frequency, ω_p, and pole Q, Q_p, using (21) and (22), respectively.

4) Determine the value of G_3 and $(G_{21}+G_{22})$ using (9) with ω_0 replaced by ω_p

$$G_3=(G_{21}+G_{22})=\omega_p\sqrt{C_1(C_{41}+C_{42})}\,.$$

(Note that here we unnecessarily exhaust one of the available degrees of freedom).

5) Rearranging (10) and replacing ω_0 by ω_p and Q by Q_p results in

$$\frac{G_{a1}+G_{a2}}{G_b}=\left(\frac{C_{41}+C_{42}}{C_1}\right)\left(\frac{G_{21}+G_{22}+G_3}{G_3}\right)-\frac{\omega_p(C_{41}+C_{42})}{Q_pG_3}. \tag{24}$$

Thus select a convenient value for G_b and use this equation to determine $(G_{a1}+G_{a2})$. For the low-pass case $G_{a2}=0$.

6) (a) For the low-pass case, use (13) to determine G_{22} and hence G_{21}. This completes the design.
(b) For the notch case, set n_1 in (12) to zero and determine G_{a2} and hence G_{a1}.
(c) For the all-pass case, divide (12) by (11) and replace (n_1/n_2) by $(-\omega_0/Q)$ and solve to determine the value of G_{a2} and hence G_{a1}. Normally G_{a1} will be very small (nominally zero).

7) Use (11) to determine the actual value of gain constant n_2.

8) Replace n_0 in (13) by $n_2\omega_z^2$ (with $\omega_z=\omega_0$ in the all-pass case, and the value of n_2 determined in step 7) above) and solve to find G_{22} and hence G_{21}.

B. Design of HPB (Fig. (3a))

1) Choose a value for Q_0 (see Section III) and use Table I to obtain nominal values for K, k and m.

2) Choose convenient values for C_{21}, C_{22}, and C_3 so that

$$\frac{C_{22}}{C_{21}} \simeq \frac{m}{1-m} \tag{25}$$

and

$$C_3 \simeq C_{21}+C_{22}.$$

To ensure solvability of design equations, (C_{22}/C_{21}) should be selected smaller or equal to the value implied by (25). If deterministic tuning in employed, the capacitor values used from here on should be the measured values.

3) Determine predistorted values for the pole-frequency, ω_p, and pole-Q, Q_p, using (21) and (22), respectively.

4) Determine the value of G_1 and $(G_{41}+G_{42})$ from (4) with ω_0 replaced by ω_p,

$$G_1=2Q_0\omega_p\sqrt{C_3(C_{21}+C_{22})}$$
$$G_{41}+G_{42}=G_1/(4Q_0^2).$$

(Note that here we unnecessarily exhaust one of the available degrees of freedom.)

For the high-pass case, $G_{42}=0$.

5) Rearranging (5) and replacing ω_0 by ω_p and Q by Q_p results in

$$\frac{G_{a1}+G_{a2}}{G_b}=\left(\frac{G_{41}+G_{42}}{G_1}\right)\left(\frac{C_{21}+C_{22}+C_3}{C_3}\right)-\frac{\omega_p(C_{21}+C_{22})}{Q_pG_1}. \tag{26}$$

Thus select a convenient value for G_b and use this equation to determine $(G_{a1}+G_{a2})$. For the high-pass case, $G_{a2}=0$.

6) (a) For the high-pass case the design is complete. Just use (6) to determine the actual value of the gain-constant n_2.
(b) For the notch case, set $n_1=0$ in (7) and obtain an equation in the two unknowns G_{a2} and G_{42}.
(c) For the all-pass case, divide (7) by (6) and replace (n_1/n_2) by $(-\omega_0/Q)$. In this way obtain an equation in the two unknowns G_{a2} and G_{42}.

7) Divide (8) by (6) and replace (n_0/n_2) by ω_z^2 (with $\omega_z=\omega_0$ in the all-pass case). In this way obtain another equation relating G_{42} and G_{a2}.

8) Solve the two linear equations obtained in steps 6) and 7) above to find G_{a2} (and hence G_{a1}) and G_{42} (and hence G_{41}).

9) Use (6) to determine the actual value of the gain constant n_2.

V. Performance Comparisons and Experimental Results

Although the above designs optimize the pole sensitivities, nothing has been said yet about the sensitivities of the transmission zeros. Changes in the transmission zeros seriously affect the transfer function of the notch and

TABLE III
SENSITIVITY COMPARISON BETWEEN LPB AND THE FRIEND LOW-PASS NOTCH CIRCUIT

Biquad #2: of / w.r.t.	ω_z	notch depth	The Friend LPN Circuit: of / w.r.t.	ω_z	notch depth
R_3	$-.5$	$* \frac{1}{2\Omega_z Q_o}$	C_3	-0.5	$-\Omega_z/(2Q_o)$
R_{22}	$\simeq -.5$	$\frac{-m}{2\Omega_z Q_o}$	C_2	-0.5	$\Omega_z/(2Q_o)$
R_{21}	very small	$\frac{-(1-m)}{2\Omega_z Q_o}$	R_3	$-0.5(1-\frac{1}{\Omega_z^2})$	$-(\Omega_z - \frac{1}{\Omega_z})/Q_o$
C_1	$-.5$	$-\frac{1}{\Omega_z Q_o}$	R_4	$-0.5/\Omega_z^2$	$-1/(\Omega_z Q_o)$
C_{42}	$\simeq -.5$	$\simeq \frac{1}{\Omega_z Q_o}$	R_{12}	$-0.5\ m$	$\frac{\Omega_z}{Q_o} + \frac{2(1-m')Q_o}{\Omega_z}$
C_{41}	very small	very small	R_{11}	$-0.5(1-m')$	$-2(1-m')Q_o/\Omega_z$
R_{a_2}	very small	$\simeq \frac{1}{\Omega_z Q_o}$	R_{b_2}	0	$-(\frac{K-k'}{K})[\frac{\Omega_z}{Q_o} + \frac{2Q_o}{\Omega_z}]$
R_{a_1}	very small	very small	R_{b_1}	0	$(\frac{1-k'}{K})[\frac{\Omega_z}{Q_o} + \frac{2Q_o}{\Omega_z}]$
R_b	very small	$\simeq \frac{1}{\Omega_z Q_o}$	R_a	0	$(\frac{K-1}{K})[\frac{\Omega_z}{Q_o} + \frac{2Q_o}{\Omega_z}]$

Note: $\Omega_z \triangleq \omega_z/\omega_o$

all-pass circuits. In this section we will investigate the sensitivities of the transmission zeros of the notch and all-pass circuits realized using the two new biquads, and provide a comparison between these and the corresponding realizations obtained using the Friend SAB. Some experimental results will be presented to verify our theoretical predictions.

A. Sensitivity Comparison with the Friend SAB

Fig. 4 shows the Friend SAB circuit which, as mentioned before, is based on a bridged-T loaded by a conductance G_3. This circuit is capable of realizing any arbitrary second-order transfer function, except for the low pass. Although detailed design equations have been provided [9], we should mention here that in the low-pass notch case $n'=0$ while in the high-pass notch case $n'=1$. To obtain a bandpass, G_3 is removed, thus reducing the SAB to the Deliyannis circuit of Fig. 1. Also, all-pass realization can be obtained by removing G_3. However, the resulting circuit has the disadvantage of having $\omega_z = \omega_0$, hence the inability to predistort for the effects of the amplifier finite bandwidth on pole frequency. If this predistortion is desired then G_3 should be left in the circuit.

Although the design optimization process described in Section III does not directly apply to the Friend SAB (in its general form) its pole sensitivities are quite comparable to those obtained in the Deliyannis bandpass and the new biquads. Furthermore, the Friend all-pass realization and the two new all-pass realizations have comparable transmission zeros sensitivities. This, however, is not the case for the notch realizations. Table III presents a summary of the sensitivities of the zero frequency ω_z and the notch depth relative to all passive components for the LPB and Friend's low-pass notch circuit. The notch depth is defined as

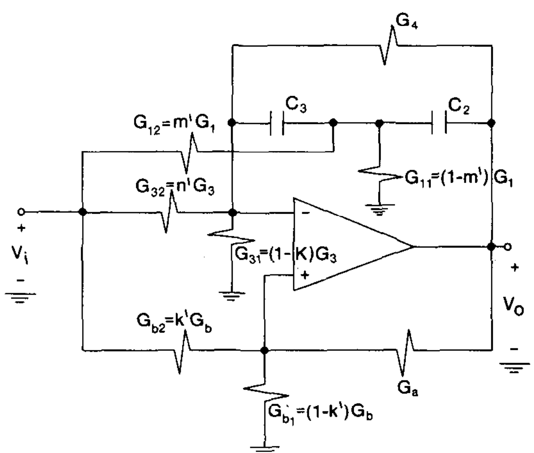

Fig. 4. The Friend SAB.

$$\text{notch depth} \equiv \frac{1}{Q_z}$$

where Q_z, ideally infinite, is the quality factor of the

TABLE IV
SENSITIVITY COMPARISON BETWEEN HPB AND THE FRIEND HIGH-PASS NOTCH CIRCUIT

Biquad #1			The Friend HPN Circuit		
of / w.r.t.	ω_z	notch depth	of / w.r.t.	ω_z	notch depth
C_3	-0.5	$-\Omega_z/(2Q_o)$	C_3	-.5	$-\Omega_z/2Q_o$
C_{22}	≈-0.5	$m\Omega_z/(2Q_o)$	C_2	-.5	$\Omega_z/2Q_o$
C_{21}	very small	$(1-m)\Omega_z/(2Q_o)$	R_3	$.5(\frac{1}{\Omega_z^2}-1)$	$-(\Omega_z-\frac{1}{\Omega_z})/Q_o$
R_1	-0.5	Ω_z/Q_o	R_4	$-\frac{1}{2\Omega_z^2}$	$-\frac{1}{\Omega_z Q_o}$
R_{42}	≈-0.5	$\approx-\Omega_z/Q_o$	R_{12}	$-.5m'$	$\frac{2Q_o}{\Omega_z}(1-m')+\frac{\Omega_z}{Q_o}$
R_{41}	very small	very small	R_{11}	$-.5(1-m')$	$-(1-m')\frac{2Q_o}{\Omega_z}$
R_{a2}	very small	$\approx\Omega_z/Q_o$	R_{b2}	$-.5(\frac{1}{\Omega_z^2}-1)$	$-(\frac{1-k'}{K})(\frac{2Q_o}{\Omega_z}+\frac{\Omega_z}{Q_o})$
R_{a1}	very small	$\approx-\frac{(K-1)(1-k)\Omega_z}{[K-k(K-1)]Q_o}$	R_{b1}	$.5(\frac{1}{\Omega_z^2}-1)$	$(\frac{1-k'}{K})(\frac{2Q_o}{\Omega_z}+\frac{\Omega_z}{Q_o})$
R_b	very small	$\approx-\frac{\Omega_z}{[K-k(K-1)]Q_o}$	R_a	very small	$(\frac{K-1}{K})(\frac{2Q_o}{\Omega_z}+\frac{\Omega_z}{Q_o})$

Note: $\Omega_z \triangleq \omega_z/\omega_o$

TABLE V
NUMERICAL SENSITIVITY COMPARISON FOR THE CASE $\Omega_z=1.2$, $Q=10$

(1) Low-Pass Biquad					(2) The Friend LPN Circuit				
of / w.r.t.	ω_o	Q	ω_z	Notch depth	of / w.r.t.	ω_o	Q	ω_z	Notch depth
R_3	-.5	0.5	-.5	0.08	C_3	-.5	0.5	-.5	-.12
R_{22}	-.17	-.17	-.5	-0.03	C_2	-.5	-.5	-.5	0.12
R_{21}	-.33	-.33	≈ 0	-0.05	R_3	≈ 0	≈ 0	-.15	-.07
C_1	-.5	-1.5	-.5	-0.16	R_4	-.5	1.5	-.35	-.17
C_{42}	-.13	0.38	-.5	0.16	R_{12}	-.13	-.39	-.13	6.4
C_{41}	-.37	1.12	≈ 0	0	R_{11}	-.37	-1.11	-.37	6.17
R_{a_2}	0	-0.45	≈ 0	0.16	R_{b_2}	≈ 0	0.25	0	-6.4
R_{a_1}	0	-0.55	≈ 0	≈ 0	R_{b_1}	≈ 0	0.75	0	6.4
R_b	0	1	≈ 0	-0.16	R_a	≈ 0	-1	0	0.08

transmission zeros. Also, the notch depth sensitivity is taken as $d[\text{Notch Depth}]/(dx/x)$. Table IV presents a similar comparison for the high-pass notch case.

Tables III and IV clearly indicated that the proposed circuits have lower notch depth sensitivities than that exhibited by the Friend circuits. This improved performance is accomplished at the expense of an additional capacitor, nevertheless the total capacitance is almost equal.

Comparing the sensitivities of LPB and HPB we note that as Ω_z increases the sensitivities of HPB increase while those of LPB decrease. For this reason we have recommended the use of HPB in the high-pass notch case and LPB in the low-pass notch case. If one is willing to accept the increase in sensitivities either circuit may be used for the entire range of Ω_z.

To gain better appreciation of the sensitivity results, numerical values are given in Table V for the case: $\omega_0=1$ rad/s, $\omega_z=1.2$ rad/s, $Q=10$, and dc gain$\simeq$0.39. For both designs a value of $Q_0=5$ was selected.

B. Experimental Verification

To verify the theoretical results given above, both types of low-pass notch circuits (LPB and Friend's) were designed, built, and tested to satisfy the following specifications

$$\omega_0=2\pi\times 4000 \text{ rad/s} \quad Q=10,$$
$$\omega_z=2\pi\times 5000 \text{ rad/s and dc gain}\simeq 0.39.$$

The design of both circuits was predistorted for $\omega_t=2\pi\times$ 750 krad/s and a value of $Q_0=5$ was used. The measured values of ω_0 and Q were as follows:

$$\text{LPB}: \omega_0=2\pi\times 4022 \text{ rad/s} \quad Q=9.86$$
$$\text{Friend Circuit}: \omega_0=2\pi\times 3978 \text{ rad/s} \quad Q=9.97.$$

To investigate the notch depth sensitivity we noted from Table V that the notch depth has the highest sensitivity with respect to

(1) R_{a2} for LPB, and
(2) R_{12} for the Friend circuit.

Therefore, the notch parameters (frequency and depth) were measured for both circuits with

(1) R_{a2} and R_{12} at their nominal values

(2) R_{a2} and R_{12} varied by -5 percent off their nominal values.

The results of these measurements are:

Circuit	R values	ω_z rad/s	Notch depth in decibels (w.r.t. dc gain)
LPB:	Nominal	$2\pi\times 4948$	-43
	-5 percent	$2\pi\times 4948$	-40
Friend's:	Nominal	$2\pi\times 4992$	-42
	-5 percent	$2\pi\times 5744$	-7.5 (!)

Thus for the realization of notch transfer functions, the new circuit is superior in performance to the Friend SAB.

VI. Conclusions

Though having similar pole sensitivities as the Friend circuits, the two biquad circuits presented display lower transmission zero sensitivities. Each of the two new circuits is capable of realizing all second-order transfer functions. However, from the point of view of lower transmission zero sensitivity, HPB should be used for the high-pass and high-pass notch functions while LPB is preferred in the low-pass and low-pass notch cases. The all-pass function may be realized with either of the two biquads. The Deliyannis circuit is the optimum configuration for realizing bandpass functions.

The design of the two biquads introduced is simple and can be optimized by directly applying the results obtained by Fleischer for the Deliyannis circuit. Also, the design is easily predistorted for the finite op amp bandwidth and deterministic tuning can be readily employed.

References

[1] K. R. Laker, R. Schaumann, and M. S. Ghausi, "Multiple-loop feedback topologies for the design of low-sensitivity active filters," *IEEE Trans. Circuits Syst.*, vol. CAS-26, pp. 1–21, Jan. 1979.

[2] A. Sedra and P. O. Brackett, *Filter Theory and Design: Active and Passive*. Portland, OR: Matrix, 1978.

[3] G. Daryanani, *Principles of Active Network Synthesis and Design*. New York: Wiley, 1976.

[4] G. S. Moschytz, *Linear Integrated Networks: Design*. New York: Van Nostrand-Reinhold, 1975.

[5] W. Saraga, "Sensitivity of second-order Sallen–Key active-*RC* filters," *Electron. Lett.*, vol. 3, pp. 442–443, 1967.

[6] A. Sedra, "Generation and classification of single amplifier filters," *Int. J. Cir. Theor. and Appl.*, vol. 2, pp. 51–67, Mar. 1974.

[7] T. Deliyannis, "High-*Q* factor circuit with reduced sensitivity," *Electron. Lett.*, vol. 4, pp. 577, 1968.

[8] J. J. Friend, "A single operational amplifier biquadratic filter section," in *1970 IEEE Int. Symp. on Circuit Theory*, (Atlanta, GA), 1970.

[9] J. J. Friend, C. A. Harris, and D. Hilberman, "STAR: An active biquadratic filter section," *IEEE Trans. Circuits Syst.*, vol. CAS-22, pp. 115–121, Feb. 1975.

[10] P. E. Fleischer, "Sensitivity minimization in a single amplifier biquad circuit," *IEEE Trans. Circuits Syst.*, vol. CAS-23, pp. 45–55, Jan. 1976.

[11] A. Sedra and L. Brown, "A refined classification of single amplifier filters," *Int. J. Circ. Theor. Appl.*, vol. 7, pp. 127–137, Mar. 1979.

[12] G. S. Moschytz and P. Horn, "Optimizing two commonly used active filter building blocks using the complementary transformation," in *Proc. 1977 Int. Symp. Circ. and Syst.*, pp. 332–335, 1977.

Adel S. Sedra (M'66), for a photograph and biography please see page 475 of the June 1980 issue of this Transactions.

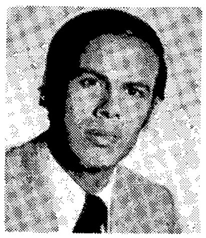

Mohamed A. Ghorab (M'78) was born in Egypt on April 17, 1936. He received the B.Sc. degree from Cairo University, Egypt, in 1958, and the Dipl. Ing. degree from the University of Delft, Holland, in 1963, both in electrical engineering.

He has held teaching and research positions with Assuit University, Egypt, and the University of Delft. In 1966, he jointed the teaching faculty of the Electrical Engineering Technology Department at Ryerson Polytechnical Institute, Toronto, Canada. In 1978, he was on a sabbatical leave at the University of Toronto, Canada, where he received the degree of Master of Engineering. His interests are in circuit theory and communication systems.

Ken Martin (S'73–M'77), for a photograph and biography please see page 244 of the April 1980 issue of this Transactions.